Moving horizon estimation of xenon in pressurized water nuclear reactors using variable-step integration

Lucas Gruss, Philippe Chevrel, Mohamed Yagoubi, Maxime Thieffry, Alain Grossetête

Moving horizon estimation of xenon in pressurized water nuclear reactors using variable-step integration

Lucas Gruss[1, 2], Philippe Chevrel[1], Mohamed Yagoubi[1], Maxime Thieffry[1], and Alain Grossetête[2]

[1]LS2N (UMR 6004), IMT-Atlantique, 4 rue Alfred Kastler 44307 Nantes, France
[2]Reactor Process Department, Framatome, 1 pl. Jean Millet 92400 Courbevoie, France

***Abstract*— A specific moving horizon estimation scheme is proposed for reconstructing the axial xenon concentrations in pressurized water nuclear reactors (PWR). The model considered is continuous time, with a parcimonious spatial discretization. The estimation scheme involves continuous time integration while using low frequency sampling of measurements. The results support a sensitivity analysis. The quality of the estimation is shown to be good, even though the model is particularly stiff, and the implementation altogether light.**

I. Introduction

A. Context

Operation of nuclear power plants (NPP) requires that many variables be kept within specific bounds in order to provide safe and efficient production of electricity. One such quantity is the build-up of xenon as a fission product. No measurement of xenon in the fuel is available.

Fission of ^{235}U produces mostly ^{135}I with rate γ_I, which β^--decays into xenon with half-life λ_I. In smaller proportions uranium directly produces xenon with rate γ_X. ^{135}Xe has a half-life of $\lambda_X = 9.2$ hours and is also transmuted into stable ^{136}Xe upon absorbing a neutron with rate σ_X, which makes it a neutron poison. The xenon/iodine equations are the following, as can be described in [1]:

$$\begin{aligned} \dot{I}(t,z) &= \gamma_I \Sigma_f \Phi(t,z) - \lambda_I I(t,z) \\ \dot{X}(t,z) &= \gamma_X \Sigma_f \Phi(t,z) + \lambda_I I(t,z) - (\lambda_X + \sigma_X \Phi) X(t,z) \, . \end{aligned} \tag{1}$$

The terms $\Gamma_I = \gamma_I \Sigma_f$ and $\Gamma_X = \gamma_X \Sigma_f$ are introduced to simplify the expressions. Σ_f depends on the cross-section of the fuel, which is dependent on the fuel cycle. $\Phi(t,z)$, $X(t,z)$ and $I(t,z)$ describe the densities in neutrons, xenon and iodine in the core as functions of time t and altitude z.

The interaction between xenon and neutron flux is to be considered in power plant operation in order to avoid a phenomenon called xenon oscillations. Such oscillations can be triggered by a small change in power distribution that alternatively causes xenon to accumulate in one part of the core and be depleted in another part. If left uncontrolled, such oscillations can diverge in a positive feedback loop and lead to safety issues.

Common ways to reduce the risks associated with xenon are appropriate control of the axial offset (AO) of power as well as sufficient downtime after shutdown. Generally, operators have to wait dozens of hours before powering up a plant again. Correct estimation of the xenon in the core can therefore provide valuable information to power producers for diagnostics, start-up and safety.

B. Contributions of the paper

In the presented work, we implement moving horizon estimation (MHE) in order to estimate the axial xenon concentration and distribution in a pressurized water reactor (PWR). The performance of MHE requires a continous-time system to be numerically integrated over "large" time intervals to account for frequently varying inputs and fast dynamics while simultaneously accomodating the slow xenon/iodine dynamics. We rely on a judicious choice of integrator to accelerate the numerical integration between the sampled measurements. This as opposed to a costlier evaluation of a high-frequency discretized model, and for better control of the integration error. We also extend previously used MHE implementations for the xenon estimation task, providing sensitivity analysis on the model parameters.

C. Related works

Estimation of xenon in nuclear reactors has been tackled both by academics and industry practitioners. The work in [2] is notable as it uses variational methods to estimate xenon in the core, which are essentially MHE methods developed by the meteorology community. It introduces two methods called "3D-Var" and "4D-var", which are moving horizon estimators with respective estimation horizon 1 and $N > 1$. The model uses 30 nodes core and includes neutronics, thermodynamics and xenon poisoning. In the same vein, we aim in the current paper to resume this work with the underlying objective of computation effort parsimony. Moreover, a sensitivity analysis of the estimator to parametric model uncertainty is proposed, which are not presented in the previous work.

The authors of [3] use Kalman filtering to carry joint state and parameter estimation on a two-points model of the core. In [4], a sliding mode observer is synthesized on the same kind of two-point model. Two-points models are the bare minimum in order to model AO of the core but are imprecise. Finer spatial discretization can help bridge the representativity gap, which is the point of the model we present. MHE proves to outperform Kalman filtering and sliding-mode observation, which motivates our choice of MHE over them.

In [5] an infinite dimension Luenberger high-gain observer is designed. The authors use a linearized model of the one-dimensional one-group diffusion equation and xenon/iodine dynamics about the steady-state xenon and flux distributions and manage to successfully reconstruct xenon, iodine and flux distributions. Our model is less conservative as we do not perform linearization. While it is interesting that the observer is designed on an infinite-dimensional model, Luenberger observers suffer from the same drawbacks as the Kalman filter and require rather strong assumptions to be applied on non-linear models.

The work in [6] addresses moving horizon estimation for singularly perturbed systems by taking a distributed approach, requiring the design of a MHE for the fast dynamics and a MHE for the "slow" dynamics. Our application is slightly different as we are not primarly interested in the fast dynamics (neutrons in our case) and focus instead on the slower dynamics of xenon. We implement and design a single estimator to estimate both slow and fast states, which is a less demanding design approach.

II. Model

We provide details on the model of the nuclear plant that will support the moving horizon estimation scheme, represented on figure 1. The reader can find more in-depth explanations on the model in [7] and [8] . The model was used for predictive control in the previous works and was validated to be a good compromise between representativity with respect to the true physics of the core and complexity. The model assumes one delayed neutron group and includes neutron diffusion equation, thermal equations, xenon/iodine dynamics and counter-reactions through moderator and doppler effects, control rods action, boron concentration and xenon poisoning. We include a modelisation of the chemical and volumetric control system (CVCS), which is responsible for the boration and dilution in the core.

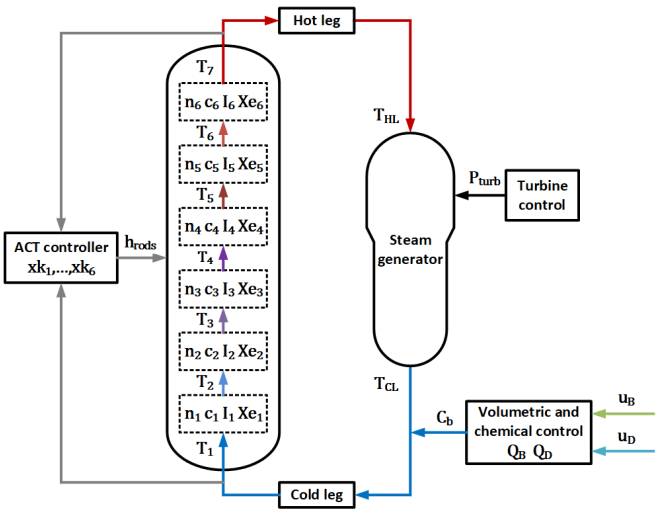

Fig. 1: Simplified model for the nuclear core, according to [7]

The model is discretized into 6 axial nodes. In each node a state comprising xenon concentration, iodine concentration, neutron power density and delayed neutrons is considered. We include temperatures between the nodes for a total of 7 temperatures, as well as the steam generator dynamics: cold and hot leg temperatures. Additionally, two boron concentrations are modeled : one for the CVCS system and one inside the core. The boron concentration in the core is considered to be uniform. The model has a total of 35 states.

Temperatures between meshes are obtained by assuming that all the power produced in the mesh is transfered to the coolant. This heat transfer is modeled through a first-order model in each node. The neutron density obeys a diffusion equation, which is implemented by considering an exchange rate D between adjacent nodes. Delayed neutrons are produced as the result of the disintegration of the fuel and other fission products with half-life β. A single delayed group is considered. Model parameters have been calibrated with the help of the neutronics codes available at Framatome.

While reactivity is usually a macro-level term in the whole core, we introduce a reactivity term in each node, which impact the neutron density in each node. This reactivity term can be broken down into five sub-terms:

- doppler anti-reactivity: depending on the local power level, the probability of fission is impacted.
- moderator anti-reactivity: a local increase in temperature in the coolant decreases the density of the water. Its ability to slow neutrons down impacts the probability of fission.
- xenon anti-reactivity: local build-up of xenon in the fuel will result in poisoning of the node, which will consume a considerable amount of neutrons, thus decreasing the number of fissions. The parameter K_X relates xenon concentration to anti-reactivity.
- boron anti-reactivity: the diluted boron absorbs neutrons and limits fissions.
- control rods anti-reactivity: the control rods contain neutron absorbing material. Inserted from the top, they locally limit the number of fissions that can happen.

We have hinted on the stiffness of the model and will expand on this topic now. The model is an ordinary differential equation, to be simulated by numerical integration. Stiffness arises from the different time-scales in the physics of the system. Xenon dynamics is orders of magnitude slower than the neutronics in the core. Integrating this model requires to use a very short integration interval in order to simulate the system. We leverage variable-step integrators as a way to speed up implementation of the estimator and limit the number of terms in the cost function.

The measurements which will be used in the cost function are 6 axial neutron flux measurements $n_{1..6}$ from excore neutronics chambers, as well as the cold leg and hot leg temperatures (T_{out} and T_{in}) of the steam generator, for a total of 8 measurements.

We consider the power extracted at the steam generator P_{turb}, control rods position h_{rods} and dilution and boration flowrates $u_{D/B}$ as inputs to the system.

III. Moving horizon estimation

A. Principles

Moving horizon estimation was proposed in [9] back in 1968, making the case for least-square optimization to solve state estimation and improve robustness to model uncertainty compared with extended Kalman filtering [10]. Kalman filtering and its variants such as the extended and "sigma-point" filters [11], [12], [13] have been the go-to techniques for non-linear estimation due to their relative ease of implementation and good practical performances. At the same time, the drawbacks are the difficulties to consider hard constraints on the estimates and in dealing with non-linearity. On the other hand, MHE can elegantly include these characteristics in the optimization problem that it solves online. Another practical advantage of MHE over other estimation techniques is explored in [14], in which MHE is shown to be an interesting choice for multi-rate and time-delayed systems.

An overview of MHE is available in [15], this estimation method has seen increasing attention thanks to model predictive control (MPC) and its breakthrough among practitioners and academia. MHE is considered to be the dual of MPC and as such most of the progress on predictive control, such as software availability and execution speed has been carried over to MHE without extra costs. Consider the following non-linear state-space model and its discretization :

$$\begin{aligned} \dot{x}(t) &= f(x(t), u(t)) \\ y(t) &= h(x(t), u(t)) \end{aligned} \Rightarrow \begin{aligned} x_{k+1} &= \Phi(x_k, u_k) \\ y_k &= h(x_k, u_k)\ . \end{aligned} \tag{2}$$

Moving horizon estimation is most often formulated in discrete-time so it is convenient to introduce a discretization of the model, which can be obtained from numerical or exact integration. At each time $t_k = k \times dt$, past measurements $[y_{k-N+1}, ..., y_k]$ and inputs $[u_{k-N+1}, ..., u_{k-1}]$ are used to estimate all the past states in $[t_{k-N+1}, t_k]$. Hence, at time t_k, N estimates of the state are produced. We introduce the notation $\hat{x}[k-i|k],\ \forall i \in [0, N-1]$ to designate the state estimates obtained from running the MHE at time t_k and $\hat{X}_k = \{x[k-N+1|k]\ \dots\ x[k|k]\}$ is the set of all estimates produced. $\overline{x}_{k-N+1}$ is a prior estimate of the beginning of the estimation window. The following optimization problem is solved online:

$$\begin{aligned} \min_{\hat{X}_k} J = &\sum_{i=0}^{N-1} \|w_i\|_Q^2 + \sum_{i=0}^{N} \|v_i\|_R^2 \\ &+ \|\hat{x}[k-N+1|k] - \overline{x}_{k-N+1}\|_{S_k}^2 \\ st.\quad w_i &= \hat{x}[k-i+1|k] - \Phi(\hat{x}[k-i|k], u_{k-i}) \\ v_i &= y_{k-i} - h(\hat{x}[k-i|k], u_{k-i}) \\ x[i] &\in \mathbb{X},\ u[i] \in \mathbb{U},\ w[i] \in \mathbb{W},\ v[i] \in \mathbb{V}\ . \end{aligned} \tag{3}$$

The estimation window is shifted forward in time as new measurements are available on the system, and a new optimization problem is solved. Three terms can be outlined from the cost function:

- The term $\sum_{i=0}^{N-1} \|w_i\|_Q^2$ is optionnal depending on the implemented algorithm. It is used when state disturbances are considered. Confidence in the model is tuned through the matrix Q: if confidence is lower the contribution of this term in the cost function should be lower, and conversly.
- The second term $\sum_{i=0}^{N} \|v_i\|_R^2$ is used to compare the estimates with the available measurements on the system, weighted with matrix R which tunes the confidence in the measurements.
- The term $\|\hat{x}[k-N+1|k] - \overline{x}_{k-N+1}\|_{S_k}^2$ is called "arrival cost". Ideally, the data used for filtering would go consist in all past measurements available on the system. This estimation scheme is called Full Information Estimation (FIE) [15]. In practice, both memory and computation requirements would grow too large to solve the problem in finite-time. Therefore in MHE, a finite-sized window of past measurements is introduced. The arrival cost can be seen as a way to "approximate" the rest of the cost function of FIE. Important results on stability and robustness of MHE depend on the design of the arrival cost, especially when the system is only detectable.

We present a common implementation of the arrival cost. Consider $\overline{x}_{k-N+1} = \hat{x}[k-N+1|k-1]$, obtained at the previous MHE step as prior estimate. The term S_k is given by running an extended Kalman filter in parallel, setting $S_k = P_k^{-1}$ where P_k is the solution to the Riccati Equation associated with the EKF. Since P_k approximates the covariance $cov(\epsilon_k)$ of the estimation error ϵ_k, S_k gives the confidence level in the previous estimation. The usual limitations on the EKF apply here, since P_k is only a local approximation of $cov(\epsilon_k)$ of the actual state. The other common issue of the EKF is that the estimation error is assumed to be gaussian whereas transformation of white noise by a nonlinear function is not gaussian in the general case. Other methods to compute the arrival cost are explored in [16], comparing EKF, UKF and particule filter. In [17], the arrival cost is computed using adaptive estimation techniques. It should also be noted that stability of MHE can be ensured even with a choice of a constant value for S_k (diagonal in the proof in [18]).

Under mild assumptions on uncertainties and noise (boundedness and compactness) [18], the estimation scheme shows good stability and robustness properties that make this method attractive despite the associated costs in computation. Efforts to reduce the computational burden leverage sensitivity results from non-linear programming, leading to implementations using suboptimal optimization [18], real-time iteration [19] or "one-step" MHE [20].

B. A formulation for stiff systems

The dynamics of xenon is slow, due to the half-lives of ^{135}Xe and ^{135}I in the range of several hours. Such time constants call for long estimation windows. In doing so, we can have significant contribution of the xenon effect in the estimation scheme, whereas shorter windows will imply less xenon variation over time, which discards the xenon dynamics. In [21], the author use an estimation horizon of two hours with successful xenon estimation.

Input signals applied to the system have faster frequency rates than the xenon dynamics and impact the neutron dynamics. Assuming a discretization of the continuous-time

model with frequency $T_s \sim 1$s would imply $N >> 1$ to achieve horizons in the range of mere minutes. This is not desirable as the optimization problem would be difficult to solve in a short timespan. Because of the slow dynamics of xenon, such a fast-paced estimator is not necessary anyway.

As such, we have to alter the MHE formulation we presented in the previous section. The estimated states in the estimation window are the result of a numerical simulation instead of a discretized model.

$$x_{k+1} = x_k + \int_{t_k}^{t_{k+1}} f(x(\tau), u(\tau))d\tau \tag{4}$$

$$y_k = h(x_k, u_k)\ . \tag{5}$$

Since the model is stiff, we use a variable-step numerical integrator between the considered measurement instants and let the integrator choose appropriate time-steps. This implementation imposes that the input signals are to be interpolated at the right time-steps, but ensures a correct input value is used. The integration error is controlled thanks to adaptive schemes, which is essential when long estimation windows are considered.

We assume that the design model is purely deterministic, that is, without process noise. This hypothesis is consistent with the first validation step, which is based on this model. That being said, most of the noise contributions are precisely known on a real installation: the dilution and boration rates are well known, the power extracted from the steam generator is known and the position of the rods is well controlled in normal operation. We also assume that only the beginning of the window is estimated, the remainder of the window can be obtained through integration. Under the previous considerations, MHE is formulated as:

$$\begin{aligned} \min_{\hat{x}[k-N+1|k]} J = &\sum_{i=0}^{N} \|v_i\|_R^2 + \|\hat{x}[k-N+1|k] - \overline{x}_{k-N+1}\|_{S_k}^2 \\ st. \quad &\hat{x}[i+1|k] = \hat{x}[i|k] + \int_{t_k}^{t_k+T_s} f(x(\tau), u(\tau))d\tau \\ &v_i = y_{k-i} - h(\hat{x}[k-i|k], u_{k-i}) \\ &x[i] \in \mathbb{X},\ u[i] \in \mathbb{U},\ v[i] \in \mathbb{V}\ . \end{aligned} \tag{6}$$

The estimation horizon is a tuning parameter for design. Longer horizons mean that we include more measurements on the system in the cost function and that we are able to capture longer dynamics. The cost function becomes closer to FIE, which is desirable. At the same time, the longer the horizon, the more computation to solve the optimization problem. Horizon length has to be carefully assessed in order to reach satisfactory performances in terms of estimation and time-requirements.

In the current formulation, compared with the "usual" MHE, the designer has an additional parameter to tune: the sampling rate $T_s = t_{k+1} - t_k$ of the measurements included in the cost function. Regardless of the actual measurement rate, we can choose to downsample measurements as to control the complexity of the optimization problem. Horizon length now refers to the quantity $(N-1)Ts$, which corresponds to the actual time spanned by the estimation window, contrary to most implementations for which "N" and "horizon length" are used interchangeably. We will assess the trade-off between higher sampling rate, horizon length and computation time.

IV. Results

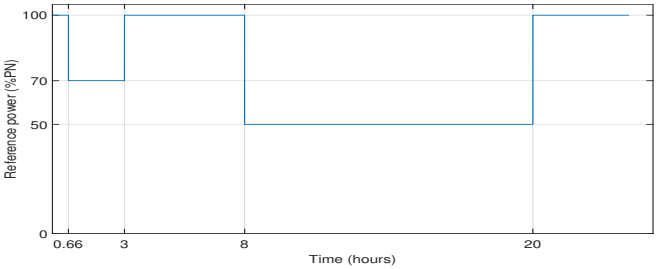

Fig. 2: Reference power throughout the validation transient

The load-follow scenario described on figure 2 is used for validation. This scenario is interesting as the successive power variations will disrupt the xenon and iodine dynamics from the equilibrium. Simulation data is representative of actual plant operation as it is obtained in closed-loop using the predictive controller in [22]. We use additive gaussian noise on the measured output, standard deviation for temperature measurements and neutron power being $\sigma_t = 0.5$ and $\sigma_n = 0.2$ respectively. Arrival cost is implemented through the constant matrix P. The weigting matrices are :

$$R = \begin{bmatrix} \sigma_t I_2 & 0 \\ 0 & \sigma_n I_6 \end{bmatrix}^{-1}$$

$$P^{1/2} = \begin{bmatrix} I_{12} & 0 & 0 & 0 & 0 \\ 0 & 10^2 I_9 & 0 & 0 & 0 \\ 0 & 0 & 10^3 I_2 & 0 & 0 \\ 0 & 0 & 0 & 10^5 I_6 & 0 \\ 0 & 0 & 0 & 0 & I_6 \end{bmatrix}^{-1} .$$

The estimator is initialized with an erroneous estimate $\hat{x}_0$ with 15% relative error to x_0, the true initial state. Boron concentration is the only exact initial estimate. Boron absorbs neutrons therefore on the dynamics of the core is similar to xenon. Our tests show that convergence is much slower when starting from an erronated boron concentration. We choose to initialize with a known value, which is a reasonable hypothesis as measurements of the boron concentration are available. Other states could be initialized similarly but do not impact the convergence of the estimator as much as boron.

Relative normalized error $\epsilon_k^{(rel)}$ on the whole state is a weighted norm using $P^{1/2}$ so that states have similar contributions to the error, despite their difference in scale (7). For other states we compute the relative error $\epsilon_{i,k}^{(rel)}$ with respect to the quantity $i \in \{X, I, T, C_b, n, c\}$ (8).

$$\epsilon_k^{(rel)} = \frac{\|P^{1/2}(\hat{x}[k|k+N-1] - x_k)\|}{\|P^{1/2} x_k\|}\ , \tag{7}$$

$$\epsilon_{i,k}^{(rel)} = \frac{\|\hat{x}_i[k|k+N-1] - x_{i,k}\|}{\|x_{i,k}\|}. \quad (8)$$

Implementation relied on `MATLAB`® [23], using `fmincon` (MATLAB Optimization Toolbox™) with interior-point algorithm to solve the non-linear optimization problem. Numerical integration of the model was handled by the variable-step integrator `ode15s`. Consumer-grade hardware was used, consisting of an `Intel`® Core™ i5-8365U CPU clocked at 1.6GHz and 16Gb of DDR4 RAM. We provide the average MHE iteration time $\bar{t}_{iter}$, which is the average solution time of each optimization problem over the 24h long transient.

A. *Trade-off between measurement rate and horizon size*

The first validation on the estimation scheme supposes no model mismatch between the design and validation model. We want to assess the tradeoff between horizon length, measurement rate and computation effort. Table I shows the results from running the estimator with different tuning parameters.

TABLE I: Comparison of different MHE tuning

Experiment #	N	Ts (s)	$(N-1)T_s$ (s)	$\bar{t}_{iter}$(s)
1	5	300s	1200	7.1
2	9	150s	1200	8.6
3	5	150s	800	5.1
4	5	600s	2400	12.1
5	9	300s	2400	10.3

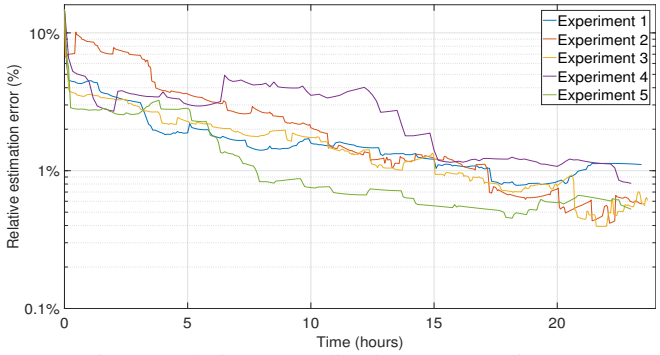

Fig. 3: Relative normalized state error (in %)

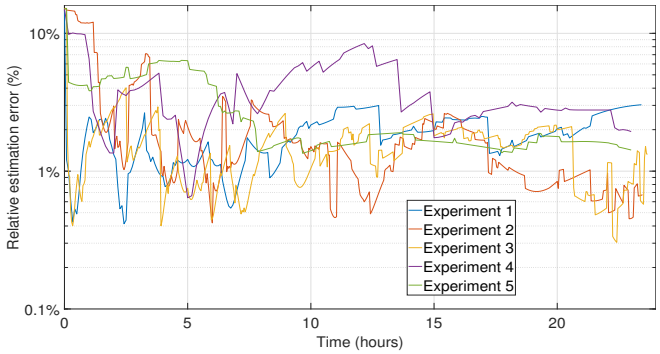

Fig. 4: Relative xenon error (in %)

We see that all estimators are able to reconstruct the state from the noisy measurements (figure 3), with a final relative normalized error $\epsilon_{final}^{(rel)}$ ranging between 0.5% and 1.1%. Focusing on the estimation of xenon, on figure 4, we observe the error decreasing very rapidly in the first iterations of MHE, due to the fact that xenon strongly impacts the dynamics. Experiment 5 yields the best results on relative normalized estimation error. This is to be expected since the horizon in this setting is longer than the others; estimation error at the beginning of the window accumulates in the cost function. When running the same experiments without measurement noise, this difference is even more noticeable. Experiment 4 shows that choosing a "long" horizon is not sufficient, only having half the sampling frequency as experiment 5 while performing significantly worse. We could expect longer horizons to imply significantly longer execution times. It is not the case, showing that the numerical integrator is very effective at choosing the appropriate time-steps, speeding up the evalution of the cost function. The result is a performant MHE execution regardless of the choice of horizon length and sampling period.

B. *Sensitivity analysis: a multi-model approach*

We assess the robustness of the estimator to model uncertainties. We consider a multi-model approach, in which different models will support MHE, each slighly off from the actual system. As we focus on the xenon/iodine dynamics, we only consider the parameters associated with it. We refer the reader to sections I and II where the parameters are introduced. Table II contains the different model mismatch situations and the error that was introduced on each parameter. Empty entries mean that nominal value was used. The MHE uses the same parameters as experiment 1, as we found that these values produced the best results in this case.

TABLE II: Sensitivity analysis of the estimator

Experiment #	β	K_X	Γ_X	σ_X	$\bar{t}_{iter}$(s)
6				-10%	9.1
7			-10%		8.4
8		+5%			6.2
9		+5%	-10%		6.6
10	+10%				6.3

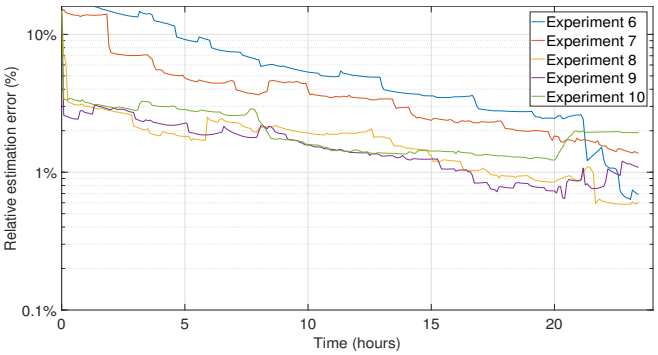

Fig. 5: Relative normalized state error (in %) with model mismatch

Robustness of the estimator to parameter uncertainty appears from figure 5. In all situations, $\epsilon_{final}^{(rel)} < 2\%$, while xenon itself is estimated to within an acceptable error level (figure 6): even the worst case scenario (experiment 7) provides

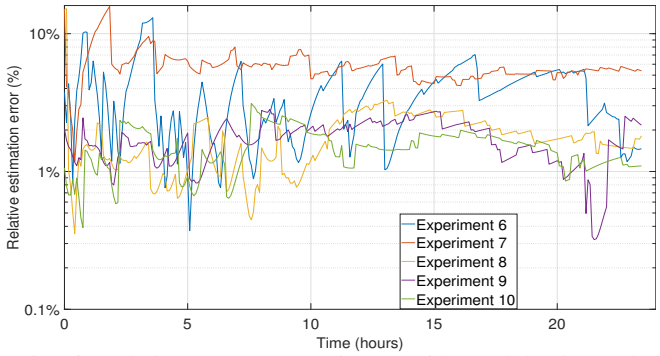

Fig. 6: Relative xenon error (in %) with model mismatch

xenon estimations such that $\epsilon^{(rel)}_{X,final} < 6\%$. Considering noises on the measurements and the stiff nature of the system, we deem this loss of estimation quality acceptable for real-world application, falling below the noise level of the available measurements.

V. Conclusions

We have designed and implemented a moving horizon estimator for xenon concentration in pressurized water nuclear reactors. The proposed scheme calls for an adapted implementation, taking advantage of variable-step integration. This makes it capable of operating in practise, both because of the quality of the estimate produced, and the computational cost required. Robustness to parameter uncertainties was confirmed through a multi-model sensitivity analysis. This supports suitability of the estimator for real-world applications.

References

[1] P. Reuss, *Précis de neutronique*. EDP Sciences, 2012.
[2] A. Ponçot, J.-P. Argaud, B. Bouriquet, P. Erhard, S. Gratton, and O. Thual, "Variational assimilation for xenon dynamical forecasts in neutronic using advanced background error covariance matrix modelling," *Annals of nuclear energy*, vol. 60, pp. 39–50, Oct. 2013,
[3] C. Lin and Y.-J. Lin, "Control of spatial xenon oscillations in pressurized water reactors via the kalman filter," *Nuclear science and engineering*, vol. 118, no. 4, pp. 260–267, Dec. 1994,
[4] G. R. Ansarifar, M. H. Esteki, and M. Arghand, "Sliding mode observer design for a PWR to estimate the xenon concentration & delayed neutrons precursor density based on the two point nuclear reactor model," *Progress in nuclear energy*, vol. 79, pp. 104–114, Mar. 2015,
[5] Y. H. Park and N. Z. Cho, "Estimation of neutron flux and xenon distributions via observer-based control theory," *Nuclear science and engineering*, vol. 111, no. 1, pp. 66–81, 1992,
[6] X. Yin and J. Liu, "Distributed moving horizon state estimation of two-time-scale nonlinear systems," *Automatica*, vol. 79, pp. 152–161, May 2017,
[7] G. Dupre, P. Chevrel, M. Yagoubi, and A. Grossetete, "Design and comparison of two advanced core control systems for flexible operation of pressurized water reactors," *Control engineering practice*, 2022,
[8] L. Lemazurier, "Conception d'un système avancé de réacteur PWR flexible par les apports conjoints de l'ingénierie système et de l'automatique," PhD thesis, Ecole nationale supérieure Mines-Télécom Atlantique, 2018.
[9] A. Jazwinski, "Limited memory optimal filtering," *IEEE transactions on automatic control*, vol. 13, no. 5, pp. 558–563, Oct. 1968,
[10] R. Kalman, "A new approach to linear filtering and prediction problems," *Journal of basic engineering (ASME)*, vol. 82D, pp. 35–45, Mar. 1960,
[11] R. Van Der Merwe, E. Wan, and S. Julier, "Sigma-point kalman filters for nonlinear estimation and sensor-fusion: Applications to integrated navigation," Aug. 2004.
[12] S. J. Julier and J. K. Uhlmann, "New extension of the kalman filter to nonlinear systems," in *Signal processing, sensor fusion, and target recognition VI*, Jul. 1997, vol. 3068, pp. 182–193.
[13] M. Nørgaard, N. K. Poulsen, and O. Ravn, "New developments in state estimation for nonlinear systems," *Automatica*, vol. 36, no. 11, pp. 1627–1638, Nov. 2000,
[14] R. Dubois, S. Bertrand, and A. Eudes, "Performance evaluation of a moving horizon estimator for multi-rate sensor fusion with time-delayed measurements," in *2018 22nd international conference on system theory, control and computing (ICSTCC)*, Oct. 2018, pp. 664–669.
[15] J. Rawlings, D. Mayne, and D. Moritz, *Model predictive control: Theory, computation, and design*, vol. 2. Nob Hill Publishing Madison, WI, 2017.
[16] S. Ungarala, "Computing arrival cost parameters in moving horizon estimation using sampling based filters," *Journal of process control*, vol. 19, no. 9, pp. 1576–1588, Oct. 2009,
[17] G. Sanchez, M. Murillo, and L. Giovanini, "Adaptive arrival cost update for improving moving horizon estimation performance," *ISA transactions*, vol. 68, Mar. 2017,
[18] A. Alessandri, M. Baglietto, G. Battistelli, and V. Zavala, "Advances in moving horizon estimation for nonlinear systems," in *49th IEEE conference on decision and control (CDC)*, Dec. 2010, pp. 5681–5688.
[19] M. Vukov *et al.*, "Real-time nonlinear MPC and MHE for a large-scale mechatronic application," *Control engineering practice*, vol. 45, pp. 64–78, Dec. 2015,
[20] P. Kã and M. Diehl, "A real-time algorithm for moving horizon state and parameter estimation," *Computers and chemical engineering*, p. 13, 2011.
[21] A. Ponçot, "Assimilation de données pour la dynamique du xénon dans les cœurs de centrale nucléaire," PhD thesis, Institut National Polytechnique de Toulouse, 2008.
[22] G. Dupré, A. Grossetête, P. Chevrel, and M. Yagoubi, "Enhanced flexibility of PWRs (mode a) using an efficient NMPC-based boration/dilution system," in *2021 european control conference (ECC)*, Jun. 2021, pp. 1092–1098.
[23] MATLAB, *Version 9.11.0 (r2021b)*. Natick, Massachusetts: The MathWorks Inc., 2021.